

Modeling of optical absorption in conjugated polymer/fullerene bulk-heterojunction plastic solar cells

H. Hoppe^{a,*}, N. Arnold^b, D. Meissner^{a,c}, N.S. Sariciftci^a

^aLinz Institute for Organic Solar Cells (LIOS), Physical Chemistry, Johannes Kepler University, Altenbergerstr. 69, 4040 Linz, Austria

^bAngewandte Physik, Johannes Kepler University Linz, Altenbergerstr. 69, 4040 Linz, Austria

^cFachhochschule Wels, Roseggerstr. 12, 4600 Wels, Austria

Abstract

To determine the actual absorption in the photoactive layer of a plastic solar cell, e.g. consisting of blend of poly(2-methoxy-5-(3,7-dimethyloctyloxy)-1,4-phenylene vinylene) (MDMO-PPV) and a methanofullerene, [6,6]-Phenyl C₆₁-butyric acid methyl ester (PCBM), a matrix formalism for the light propagation in this multi-layer system is applied. This calculation results in an upper limit for the incident photon to collected electron (IPCE) conversion efficiency for a given internal quantum efficiency. Comparisons with experimental results as well as conclusions for the optimal layer thickness are drawn.

© 2003 Elsevier B.V. All rights reserved.

Keywords: Optical modeling; Plastic solar cell; Absorption; Refractive index; Internal quantum efficiency

1. Introduction

Thin film organic solar cells based on conjugated polymer/fullerene blends experienced increasing research interest within the past few years [1–3]. One main progress in terms of solar energy conversion efficiency has been achieved by introducing the bulk-heterojunction concept [4–7] instead of the bilayer structure [8–11] for the photoactive layer. The highly increased interfacial area between the donor and acceptor phases characterizes a bulk-heterojunction. This enables photoinduced charge separation [12] even within the bulk of the photoactive layer, instead of just at the thin planar interface. Assuming a sufficiently fine intermixing, all photons absorbed within the photoactive layer may contribute to the charge generation. In contrast, only excitons generated closely enough to the bilayer junction could contribute to charge generation in the bilayer devices. Hence optical modeling was applied to place the electric field maximum at the interface of the two layers [13–16].

Recently, Shaheen et al. [7] reported 2.5% AM 1.5 solar conversion efficiency for a bulk-heterojunction device consisting of a blend of poly(2-methoxy-5-(3,7-

dimethyloctyloxy)-1,4-phenylene vinylene) (MDMO-PPV) and a fullerene C₆₀-derivative 1-(3-methoxycarbonyl) propyl-1-phenyl [6,6]C₆₁ (PCBM). From reflection and incident photon to collected electron (IPCE) measurements, the authors estimate the internal quantum efficiency to be approximately 85%. The fraction of the incident photons that are absorbed within the photoactive layer is in fact an unseizable magnitude. The knowledge of this absorbed fraction enables to connect the external quantum efficiency (EQE, corresponds to IPCE) with the internal. Here we report on the optical modeling of devices based on MDMO-PPV and P3HT (regioregular-(poly(3-hexylthiophene-2,5-diyl))) mixed with PCBM, to determine the part of the light, which is absorbed within the active layer.

2. Experimental

2.1. Methods

For modeling of light propagation within the solar cell device, the complex refractive indices of all involved layers needed to be determined (see [17]). Hence, near normal incidence (7°) transmission and reflection spectra of spin cast films on fused silica and of the ITO-substrate were recorded using a Cary 3G spectrophotometer (Varian, Inc., Palo Alto, USA) in the

*Corresponding author. Tel.: +43-732-2468-8854; fax: +43-732-2468-8770.

E-mail address: harald.hoppe@jku.at (H. Hoppe).

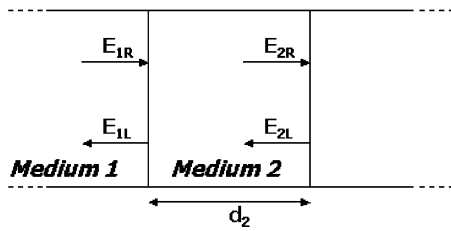


Fig. 1. Schematic for the transfer matrix formalism. E_{iR} and E_{iL} are the electric field amplitudes in the i th layer propagating in the right and left direction, and d_2 denotes the thickness of layer 2.

range between 300 and 900 nm. The organic layer thickness was verified using a tapping mode AFM (Dimension 3100, Digital Instruments, Santa Barbara, USA), by measuring the depths of scratches in the film. The complex refractive index $\tilde{n} = n + ik$ is achieved by fitting a complex model dielectric function $\tilde{\epsilon} = \epsilon' + i\epsilon''$ to the respective transmission and reflection spectra by using the software SCOUT2 (M. Theiss, Aachen, Germany). The model dielectric function is built of a constant dielectric background (contributing to its real part) and of so-called Kim-oscillators [18], which describe the optical absorption for the electronic transitions by any line-shape between a Gaussian and a Lorentzian profile. The relations between the complex refractive index and the dielectric function are given by: $\epsilon' = n^2 - k^2$ and $\epsilon'' = 2nk$.

To model the optical properties of our multilayer system, the so-called transfer matrix formalism (TMF) is applied [13,19–21]. Here the multilayer is treated as a one-dimensional system in which the amplitude of the electromagnetic field vector is calculated coherently, i.e. considering the phase. This formalism considers two electromagnetic waves, one propagating in the positive direction (E_{iR}) perpendicular to the interfaces of the multilayer system, and one in the opposite direction (E_{iL}), see Fig. 1). By traveling from layer 1 to layer 2, the wave undergoes Fresnel reflection and transmission, while within a layer the propagation leads to some phase shift of the wave and decay according to the absorption of the material. All, the reflection, the transmission, the phase shift and the absorption can be described in terms of the optical constants n and k . The change of phase and amplitude can thus be written as a 2×2 matrix, treating both, the forward and backward propagation direction:

$$\begin{bmatrix} E_{iR} \\ E_{iL} \end{bmatrix} = \frac{1}{t_{12}} \begin{bmatrix} e^{-i\delta_2} & -r_{12}e^{i\delta_2} \\ -r_{12}e^{-i\delta_2} & e^{i\delta_2} \end{bmatrix} \times \begin{bmatrix} E_{2R} \\ E_{2L} \end{bmatrix} = \frac{1}{t_{12}} M_{12} \begin{bmatrix} E_{2R} \\ E_{2L} \end{bmatrix},$$

where

$$\delta_2 = \frac{2\pi}{\lambda} n_2 d_2. \quad (1)$$

By multiplying these matrices for the involved layers, the amplitude and phase of the electric field are known within the system at any point and the local absorption can be calculated. The optical modeling has been performed for a cell structure as shown in Fig. 2. More details on the modeling can be found in Hoppe et al. [22].

2.2. Materials and films

MDMO-PPV was provided by Covion (Germany), PEDOT:PSS (poly[3,4-(ethylenedioxy) thiophene]:poly(styrene sulfonate)) (Baytron) by Bayer (Germany) and PCBM was purchased from J.C. Hummelen (University of Groningen, The Netherlands). Films were prepared by spin coating from chlorobenzene solutions of 1:4 (by weight) blends of MDMO-PPV and PCBM. Regioregular-P3HT (poly(3-hexylthiophene-2,5-diyl)) was purchased from Rieke Metals Inc. (Nebraska, USA) and films were spin cast from ortho-dichlorobenzene in a blend with PCBM at a ratio of 1:2 (by weight). PEDOT:PSS was spin cast from an aqueous solution with a concentration of 0.5% by weight. As a substrate, fused silica cleaned with iso-propanol in an ultrasonic bath before spin coating was used. In order to determine the optical constants of both layers of the ITO-glass (MERCK, Germany), on one sample the transparent indium tin oxide (ITO) was etched away completely in a mixture of conc. HNO_3 , conc. HCl and distilled H_2O in a ratio of 1:9:10 by volume to allow for the determination of the optical properties of the substrate glass alone. To form the back contact for the devices, approximately 0.6 nm LiF and 70 nm aluminum were thermally evaporated onto the active layer.

3. Results and discussion

In Fig. 3, the results for the optical modeling of a device consisting out of 1.1 mm glass, 125 nm ITO, 75



Fig. 2. Schematic structure of the modeled multilayer device. The incoming light (I_{in}) enters the device and propagates attenuated towards the aluminum electrode. There it is reflected and the outgoing intensity (I_{out}) leaves the device through the glass. Due to the high reflectivity and absorption of the sufficiently thick aluminum electrode, no light leaves or enters from the right side of the device.

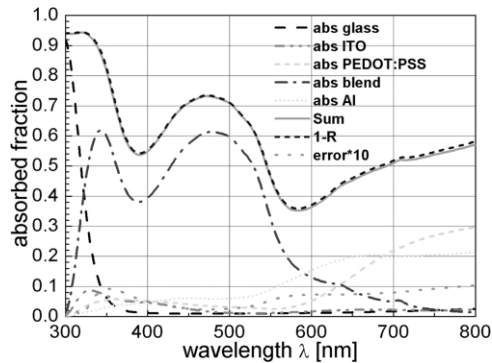


Fig. 3. The wavelength-dependent fractions of the light, which are absorbed in each layer of the solar cell device, are depicted. Note the good agreement between the summated absorbed fractions, total absorbance A and $1-R$.

nm PEDOT:PSS, 90 nm active layer (MDMO-PPV:PCBM 1:4) and a sufficient thick aluminum back contact to absorb any light that is reaching it, are presented. Depicted is the fraction of the incident intensity that is absorbed within each layer at the different wavelengths of the light. In addition, the result for the device reflection R is shown, which is a direct result of the TMF. We find a very good agreement between the summated absorption and $1-R$, thus the relation $A+R=1$ is valid (A being the absorption of the multilayer). If the absorption for the active layer is folded with the normalized AM 1.5 solar spectrum, predictions for the maximum short circuit current I_{SC} can be made. In Fig. 4, the results for the variation of the active layer thickness—consisting of the MDMO-PPV:PCBM 1:4 blend—are shown. Interestingly, we find a shallow local maximum of the predicted current at approximately 90 nm and the function of the max. I_{SC} is rather wavy depending on the active layer thickness. We assign this directly to interference effects in the whole device, which may lead to an optimized overlap between the 90-nm active layer absorption and the solar spectrum. In general, we do have an increasing possible photocurrent for a larger active layer thickness, but the limited conductivity of the organic layer and thus recombination is expected to knock down real photocurrents at increasing active layer thicknesses. From the calculation for the 100 nm device, assuming the open circuit voltage V_{OC} and the fill factor FF to be the same as reported in [7], we find the internal quantum efficiency IQE of the measured device to be larger than 80%. This shows a rather good agreement between experimental photocurrents and simulated absorption for the active layer.

Recently, there have been reports on P3HT based solar cell devices of having 70% and more external quantum efficiency (EQE) as peak values [23,24]. In Ref. [24] the authors account the increased device efficiency due to annealing and applying of a forward

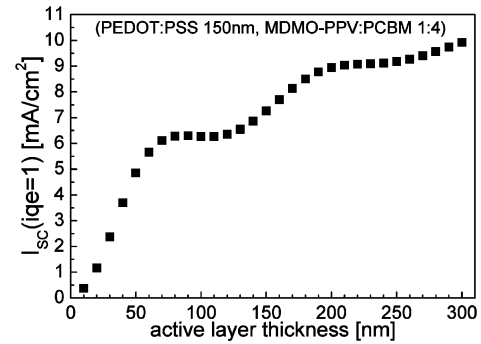


Fig. 4. Calculated short circuit current for different (MDMO-PPV:PCBM 1:4) active layer thicknesses assuming an internal quantum efficiency of unity. The PEDOT layer thickness is set to 150 nm.

current after the production of the whole device to be mainly due to burning of shunts and an increase in the charge carrier mobility. In Fig. 5 the results from Ref. [24] are reprinted, and a large effect on the IPCE or EQE due to the treatments is visible. In this work, we want to quantify the gain for the maximum photocurrent due to increased absorption. Consequently, P3HT:PCBM (1:2) devices have been prepared with cell areas of approximately 1 cm^2 , where one sample was left untreated, while the others were treated according to Ref. [24]. In Fig. 6, the results for the measured and fitted reflectivities are depicted. The optical properties, respectively, the dielectric functions of the photoactive layer were adjusted in this fitting, while the dielectric functions of the other layers were already determined earlier, separately. Here the active layer thickness in the modeling was kept constant at 72 nm, close to the experimental values from AFM measurements of single films on glass. From the optical modeling we get the fraction

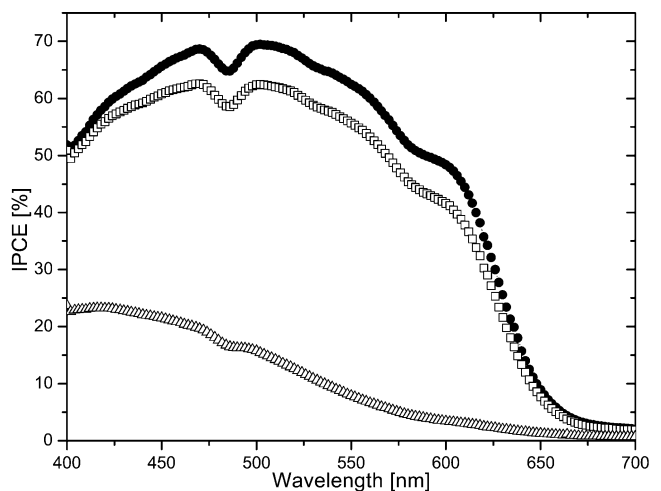


Fig. 5. IPCE curves of P3HT:PCBM solar cells for different treatments: non-treated (Δ), annealed (\square) and annealed and voltage applied (\bullet). Reprinted from [24].

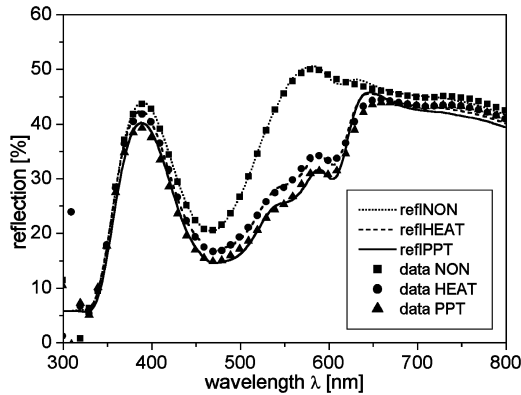


Fig. 6. Reflection of whole solar cell devices for different treatments: non-treated (dots and squares), annealed (dashes and circles) and annealed and voltage applied (triangles and full line). The respective lines show the fit results for the measured data (points).

of the light, which is absorbed in the active layer (Fig. 7) and by folding with the AM 1.5 solar spectrum maximum photocurrents are deduced. As results, the non-treated device predicted 6.34 mA/cm^2 , the annealed sample 8.42 mA/cm^2 and the annealed and biased sample 9.02 mA/cm^2 . Comparing these numbers with the measured IPCE spectra indicates that the optical effects of the treatment cannot account for the increased device efficiency alone, but they may contribute to the maximum photocurrent by more than 40%.

4. Conclusions

Optical modeling is a valuable tool to quantify optical losses and gains within thin film organic photovoltaic devices. This procedure shows for MDMO-PPV based plastic solar cells, that a local optimum of the layer thickness is approximately 90 nm, closely related to the

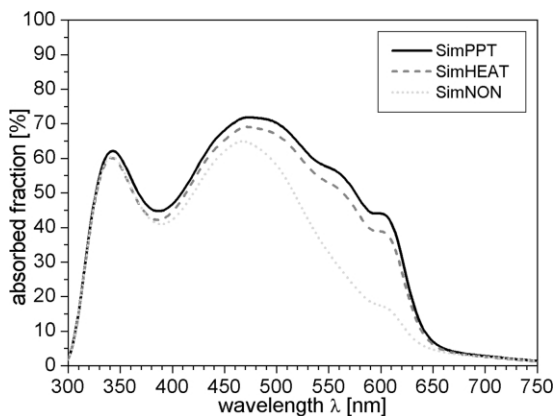


Fig. 7. Modeled optical absorption for the active layer of solar cell devices for different treatments: non-treated (dots), annealed (dashes) and annealed and voltage applied (full line).

experimentally optimized device reported in Ref. [7]. In the case of P3HT based solar cells it was shown that treatments described in Ref. [24] led to an increase in the optical absorption in the photoactive layer of more than 40%. Hence, optical gains play an important role for the increased photocurrent and device efficiency.

Acknowledgments

Our study was supported by the BMBF-project 'Erneuerbare Energien: Organische Solarzellen' (contract number 01SF0026) (Germany). We gratefully acknowledge R.S. Rittberger for technical assistance.

References

- [1] C.J. Brabec, N.S. Sariciftci, J.C. Hummelen, *Adv. Funct. Mater.* 11 (2001) 15.
- [2] V. Dyakonov, *Phys. E* 14 (2002) 53.
- [3] C.J. Brabec, V. Dyakonov, J. Parisi, N.S. Sariciftci, *Organic Photovoltaics*, Springer Series in Materials Science 60 (2003).
- [4] G. Yu, A.J. Heeger, *J. Appl. Phys.* 78 (1995) 4510.
- [5] G. Yu, J. Gao, J.C. Hummelen, F. Wudl, A.J. Heeger, *Science* 270 (1995) 1789.
- [6] J.J.M. Halls, C.A. Walsh, N.C. Greenham, E.A. Marseglia, R.H. Friend, S.C. Moratti, A.B. Holmes, *Nature* 376 (1995) 498.
- [7] S.E. Shaheen, C.J. Brabec, N.S. Sariciftci, F. Padinger, T. Fromherz, J.C. Hummelen, *Appl. Phys. Lett.* 78 (2001) 841.
- [8] C.W. Tang, *Appl. Phys. Lett.* 48 (1986) 183.
- [9] N.S. Sariciftci, D. Braun, C. Zhang, V.I. Srdanov, A.J. Heeger, G. Stucky, F. Wudl, *Appl. Phys. Lett.* 62 (1993) 585.
- [10] J.J.M. Halls, K. Pichler, R.H. Friend, S.C. Moratti, A.B. Holmes, *Appl. Phys. Lett.* 68 (1996) 3120.
- [11] L.S. Roman, W. Mammo, L.A.A. Pettersson, M.R. Andersson, O. Inganäs, *Adv. Mat.* 10 (1998) 774.
- [12] N.S. Sariciftci, L. Smilowitz, A.J. Heeger, F. Wudl, *Science* 258 (1992) 1474.
- [13] L.A.A. Pettersson, L.S. Roman, O. Inganäs, *J. Appl. Phys.* 86 (1999) 487.
- [14] J. Rostalski, *Der Photovoltaisch aktive Bereich molekularer organischer Solarzellen*, Ph.D. Thesis, Fachbereich 1, Rheinisch Westfälisch Technische Hochschule Aachen, 1999.
- [15] J. Rostalski, D. Meissner, *Sol. Energy Mater. Sol. Cells* 63 (2000) 37.
- [16] G. Meinhardt, D. Gruber, G. Jacopic, Y. Geerts, W. Papousek, G. Leising, *Synth. Metals* 121 (2001) 1593.
- [17] H. Hoppe, N.S. Sariciftci, D. Meissner, *Mol. Cryst. Liq. Cryst.* 385 (2002) 113.
- [18] C.C. Kim, J.W. Garland, H. Abad, P.M. Raccah, *Phys. Rev. B* 45 (20) (1992) 11749.
- [19] B. Harbecke, *Appl. Phys. B* 39 (3) (1986) 165.
- [20] O.S. Heavens, *Optical Properties of Thin Solid Films*, Dover Publications, New York, 1991.
- [21] Sh.A. Furman, A.V. Tikhonravov, *Basics of Optics of Multi-layer Systems*, Frontiers, Paris, 1996.
- [22] H. Hoppe, N. Arnold, N.S. Sariciftci, D. Meissner, *Sol. Energy Mater. Sol. Cells* 80 (2003) 105.
- [23] P. Schilinsky, C. Waldauf, C.J. Brabec, *Appl. Phys. Lett.* 81 (2002) 3885.
- [24] F. Padinger, R.S. Rittberger, N.S. Sariciftci, *Adv. Funct. Mater.* 13 (2003) 1.